International Journal of Chemical and Biochemical Sciences
(ISSN 2226-9614)

Journal Home page: www.iscientific.org/Journal.html

Insights into Corrosion Inhibition of Mild Steel in Hydrochloric Acid Solution by New Vitreous Phase

G. Ghenimi[1], M. Ouakki[1,3], Z. Aribou[2], H. Barebita[1], T. Guedira[1], M. Cherkaoui[1,3]*

[1]*Laboratory of Organic Chemistry, catalysis and Environment, Faculty of Sciences, Ibn Tofaïl University, PO Box 133, 14000, Kenitra, Morocco.*

[2]*Laboratory of Advanced Materials and Process Engineering, Faculty of Sciences, University Ibn Tofail PB. 133-14000, Kenitra, Morocco.*

[3]*National Higher School of Chemistry (NHSC), University Ibn Tofail BP. 133-14000, Kenitra, Morocco.*

Abstract

New glassy materials correlated with the ternary system Bi_2O_3-B_2O_3-P_2O_5, were synthesized and tested as corrosion inhibitors for mild steel in 1.0 M hydrochloric acid solution using electrochemical impedance spectroscopy and potentiodynamic polarization methods. The samples were characterized by scanning electron microscopy (SEM), and energy dispersive X-ray spectroscopy (EDX). The obtained results showed that the change in the impedance parameters with the concentration of inhibitors is indicative. The inhibitors efficiency was observed to increase with decreased concentration of 4H3BO3 and 6H3BO3 at room temperature. Inhibition efficiencies of 4H3BO3 and 6H3BO3 followed the order: 81,4% (4H3BO3) < 86.5% (6H3BO3). The inhibitors exhibited excellent performance at the studied temperatures. However, the performance decreases with an increase in temperature.

Keywords: Glassy phase, inhibition, corrosion, mild steel, HCl, EIS, SEM

Full-length article **Corresponding Author*, e-mail: *moussa.ouakki@uit.ac.ma*

1. Introduction

Annually, corrosion causes over $2.5 trillion in economic damage worldwide [1]. Due to corrosion, the main properties of mild steel are lost [2]. Corrosion of mild steel occurs in aqueous and atmospheric environments [3]. It depends on many important factors, such as temperature, pH of the corrosive solution and oxygen concentration [4]. Mild steel also corrodes during industrial applications such as pickling, acid cleaning, acidizing, crude oil transportation, heating and cooling. Corrosion of mild steel is a serious economic, environmental and industrial problem. In the fields of engineering, materials science, and chemistry, several effective methods of protecting metals from corrosion have been proposed; these methods include the use of corrosion inhibitors, galvanization, electrochemistry (anodic and cathodic protection), coatings, and painting, which are the most commonly used methods for corrosion protection.

According to the literature, several studies demonstrated that one of the most effective methods to prevent corrosion is to add inorganic corrosion inhibitors [5,6], used as inhibitors to control the corrosion process of steel in the presence of acidic solutions [7,8], such as boric acid [9], molybdate [10], phosphate [11] and glasses [12-15]. Although several inorganic inhibitors are known to be highly effective, many drawbacks limit their use because of their toxicity and high cost [16,17]. For this reason, the development of alternative inorganic inhibitors has become essential [18-21]. This requires the study of the feasibility of using new inorganic compounds derived from the oxides Bi_2O_3, Nb_2O_5, V_2O_5, and P_2O_5 which showed high inhibitory efficiency with negligible toxicity [22-24].

The aim of this paper is to evaluate the inhibition effectiveness of both glassy compounds (4H3BO3 and $6H_3BO_3$) against the corrosion of steel in molar HCl medium. the inhibitive performance of these products was investigated using PDP curves and SEM/EDS. The effect of temperature on the electrochemical parameters of the system was studied as well, in order to define the adsorption mechanism of the studied compounds.

2. Materials and methods

2.1. Inhibitor's synthesis

Glassy phosphates were prepared from bismuth oxide Bi_2O_3, boric acid H_3BO_3 and diammonium hydrogen phosphate $(NH_4)_2HPO_4$ by stoichiometric mixture of raw materials according to the following reaction (1) [25]:

$$(1\text{-}x\text{-}y)\ Bi_2O_3 - yH_3BO_3 - x\ 2[(NH_4)_2HPO_4] \rightarrow (1\text{-}x\text{-}y)\ Bi_2O_3 + y1/2B_2O_3 + xP_2O_5 \quad (1)$$

The weighed materials were mixed and crushed in an Agat mortar. The thermic operation is realized in porcelain crucibles. The first treatment at 350 °C for 15 h enables hydrogen decomposition, it is followed by a grinding for homogenization. Each reaction mixture is then melted in an oven at 1050 °C, energetically plunged into a preheated aluminum mould at 200 °C [26]; and then stored in desiccators to avoid moisture. The compositions studied are collected in Table 1.

2.2. Material and medium

The aggressive medium of 1.0 M Hydrochloric acid were prepared by dilution of HCl (37% in weight) with distilled water. The concentrations of the two compounds ranged from 50 to 300 ppm. The metal use for present study was of mild steel, with the chemical composition (in wt%) of 0.370 % C, 0.230 % Si, 0.680 % Mn, 0.016 % S, 0.077 % Cr, 0.011 % Ti, 0.059 % Ni, 0.009 % Co, 0.160 % Cu and the remainder iron (Fe). For electrochemical experiences, the mild steel substrate was used with an exposed surface of 1cm^2 to the acid medium. Before each use, the substrate was polished with emery paper from 180 to 1500, rinsed with distilled water, degreased with ethanol, and drying in hot air.

2.3. Electrochemical measurements

The electrochemical (PDP and EIS) tests were realized in a conventional three-electrode Pyrex cell are connected with the potentiostat/ galvanostat (PGZ 100) related to a computer with an analysis software model (Volta master 4). In this study, working electrode of steel substrate with an exposed area of 1 cm^2, a Pt counter electrode and an Ag/AgCl/KCl saturated reference electrode. Before starting the experiments, the working electrode was immerged in the test solutions for 30 min to attain a steady-state open circuit potential (E_{OCP}). The Tafel plots were recorded by changing the electrode potential automatically from negative values to greater ones versus E_{corr} from –900 to –100 mV/Ag/ AgCl with at a scan rate of 1 mV/s. For the temperature effect side of the present study, the testing temperatures ranged between 298 and 328 K. Inhibitive performance η(%) has been determined using the formula:

$$\eta_{pp}\% = \frac{i^0_{corr} - i_{corr}}{i^0_{corr}} \times 100 \qquad (2)$$

Where i^0_{corr} and i_{corr} stand for the values of corrosion current densities in the nonexistence and existence of inhibitor, respectively. The measurement of the electrochemical impedances was done under the same conditions as the polarization plots, at frequencies between 100 KHz and 100 mHz, using a sinusoidal disturbance potential of 10 Mv. The inhibition efficiency, derived from EIS, Heis% was also added and calculated using the following equation (2):

$$\eta_{EIS}\% = \frac{R_{ct} - R^0_{ct}}{R^0_{ct}} \times 100 \quad ; \quad \theta = \frac{R_{ct} - R^0_{ct}}{R^0_{ct}} \qquad (2)$$

Where R^0_{ct} and R_{ct} are the values of charge transfer resistance in the absence and presence of both compounds $4H_3BO_3$ and $6H_3BO_3$.

2.4. Surface characterization

The surface morphology mild steel surface characterization before and after 6 h of immersion in Hydrochloric acid 1,0 M solution, in the absence and presence of both compounds studied 4H3BO3 and 6H3BO3 at 298 K, was executed by SEM analysis using Quanta FEG 450. The elemental analysis is obtained by coupling the system with an energy dispersive analysis (EDX).

3. Result and discussion

3.1. Polarization curves

Figure 1 shows the polarization plots for mild steel in 1.0 M Hydrochloric acid with and without addition of 4H3BO3 and 6H3BO3 at 298 °K. A remarkable reduction of the cathodic and anodic current densities is observed. This result shows that the addition of these inhibitors reduces the anodic dissolution and the potential shift of the hydrogen evolution reaction. Moreover, cathodic Tafel curves give rise to parallel lines with inhibitor concentration; this shows that the addition of these inhibitors does not modify the hydrogen evolution mechanism. The reduction of H^+ ions at the mild steel surface take place mainly through a charge transfer mechanism [22,27].

$$Fe \rightleftharpoons Fe^{2+} + 2e^-$$

$$H^+_{ads} + H^+ + 2e^- \rightleftharpoons H_2$$

$$H^+_{ads} + e^- \rightleftharpoons H_{ads}$$

$$2H^+ + 2e^- \rightleftharpoons H_2$$

The electrochemical parameters such as the corrosion potential E_{corr}(mV/Ag/AgCl), the cathodic and anodic slopes βc and βa, the corrosion current density i_{corr} and the inhibition efficiency $\eta_{pp}\%$ are presented in Table 4. It can be noticed from Table 2 shows that the investigated compounds show a good inhibitory effect against the corrosion of mild steel in 1 M HCl medium. This result reveals a decrease in the corrosion current, to achieve a value, thus inhibitory efficacy is equal to 81,4% and 86,5% to 50 ppm for both 4H3BO3 and 6H3BO3 compounds respectively. The addition of the compounds in the electrolyte has also caused the variation of E_{corr} values, the displacement is superior to 85 mV, and thus, the inhibitor could be considered as a cathodic or anodic type [28-30]. If the variation is lower than 85 mV, the inhibitor can be considered as a mixed type inhibitor [31]. This result could indicate that the inhibitory action occurred simply by blocking the cathodic and anodic sites available on the surface of the metal. By adsorption of inhibitor molecules on the surface of the steel [32,33].

3.2. EIS studies

Impedance findings were analyzed by fitting these experimental data to an equivalent circuit model. Therefore, the recorded findings are listed in Table 3. As given in Fig. 2, Rs stands for the solution resistance, Rct represent the charge transfer resistance, and CPE (Q, n) denotes the constant phase element [35,36].

Table 1. Composition of glassy elements studied within the system

(1-x-y) Bi_2O_3 +y 1/2B_2O_3+ xP_2O_5			
Echa. N°	1-x-y	y	x
4H_3BO_3	0.65	0.25	0.1
6H_3BO_3	0.35	0.55	0.1

Table 2. Electrochemical parameters derived from the Tafel plots of mild steel in 1M hydrochloric acid medium before and after the addition of the glassy compounds at 298 K

Compounds	**Conc. ppm**	**-E_{corr} mV/Ag/AgCl**	**i_{corr} µA cm^{-2}**	**-β_c mV dec^{-1}**	**β_a mV dec^{-1}**	**η_{PP} %**
Blank	--	498	983	140	150	
4H_3BO_3	50	552	183	123	130	81,4
	100	540	254	126	128	74,2
	200	562	263	132	134	73,2
	300	560	285	136	140	71,0
6H_3BO_3	50	464	133	128	132	86,5
	100	515	262	125	127	73,3
	200	510	333	130	134	66,1
	300	507	362	126	138	63,2

Table 3. Electrochemical parameters derived from the EIS diagrams before and after the addition of the glassy compounds in various concentrations to corrosive solution.

	C (ppm)	**R_s (Ω cm^2)**	**R_{ct} (Ω cm^2)**	**C_{dl} (µF cm^{-2})**	**n_{dl}**	**Q (µF.S^{n-1})**	**η_{imp} %**
Blank	--	1.9	23.4	190	0.897	470	--
4H_3BO_3	50	1.1	117.4	65	0.886	210	80,0
	100	1.4	89.0	96	0.937	231	73,7
	200	1.5	87.0	112	0.890	245	73,1
	300	1.3	79.3	125	0.925	342	70,5
6H_3BO_3	50	1.5	163.0	56	0.918	206	85,6
	100	1.6	85.7	89	0.892	150	72,7
	200	1.7	68.3	115	0.867	375	65,7
	300	1.5	62.9	122	0.874	273	62,8

Table 4. Both Electrochemical and activation parameters for mild steel dissolution in acidic medium before and after protection.

Compounds	**Tempe K**	**-E_{corr} mV/Ag/AgCl**	**i_{corr} µA cm^{-2}**	**-β_c mV dec^{-1}**	**β_a mV dec^{-1}**	**η_{PP} %**
Blank	298	498	983	140	150	-
	308	491	1200	184	112	-
	318	475	1450	171	124	-
	328	465	2200	161	118	-
4H_3BO_3	298	552	183	123	130	81,4
	308	525	245	170	113	79,6
	318	518	334	166	120	76,9
	328	510	573	154	119	73,9
6H_3BO_3	298	464	133	128	132	86,5
	308	516	188	164	109	84,3
	318	499	261	159	122	82.0
	328	500	445	147	117	79,7

Table 5. The values of activation parameters Ea, ΔHa, and ΔSa for mild steel in 1.0 M HCl in the absence and presence of inhibitors.

	Ea (KJ/mol)	**ΔHa (KJ/mol)**	**ΔSa (J/mol.K)**
Blank	21.0	18.5	-126.0
$4H_3BO_3$	30.2	27.6	-109.5
$6H_3BO_3$	32.0	29.4	-105.9

Table 6. Percentage compositions of elements present on the mild steel surface.

Elements	Blank	**$4H_3BO_3$**	**$6H_3BO_3$**
C	4.9	3.4	3.5
O	19.3	2.9	2.8
P	--	0.04	0.09
Bi	--	8.12	6.27
Fe	75.8	85.54	91.7

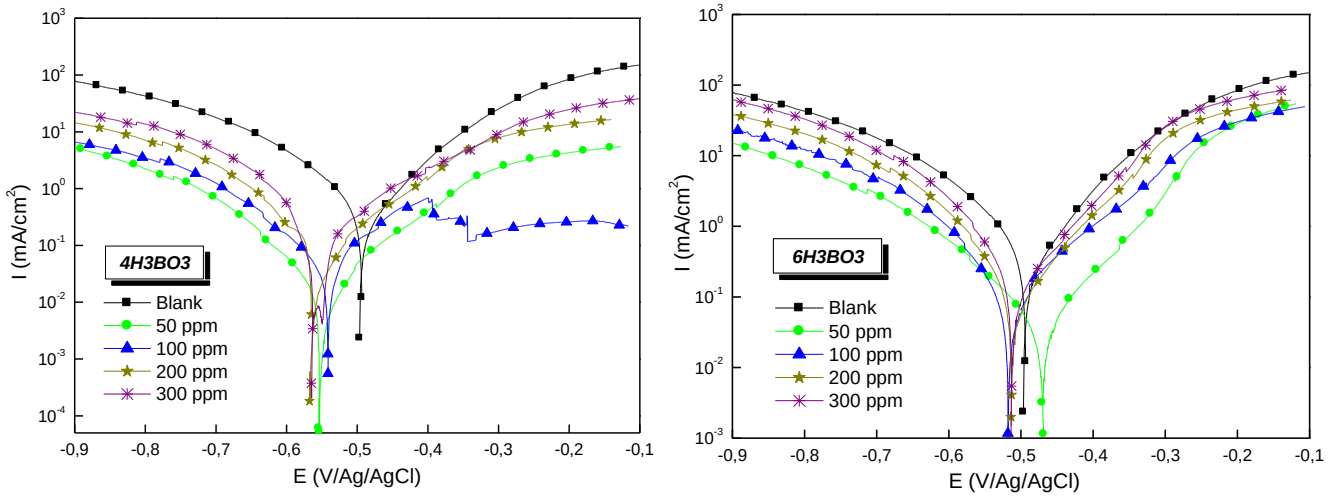

Fig. 1. Polarization plots for mild steel in 1.0 M HCl in the absence and presence of the glassy compounds $4H_3BO_3$ (a) and $6H_3BO_3$ (b) at 298 K

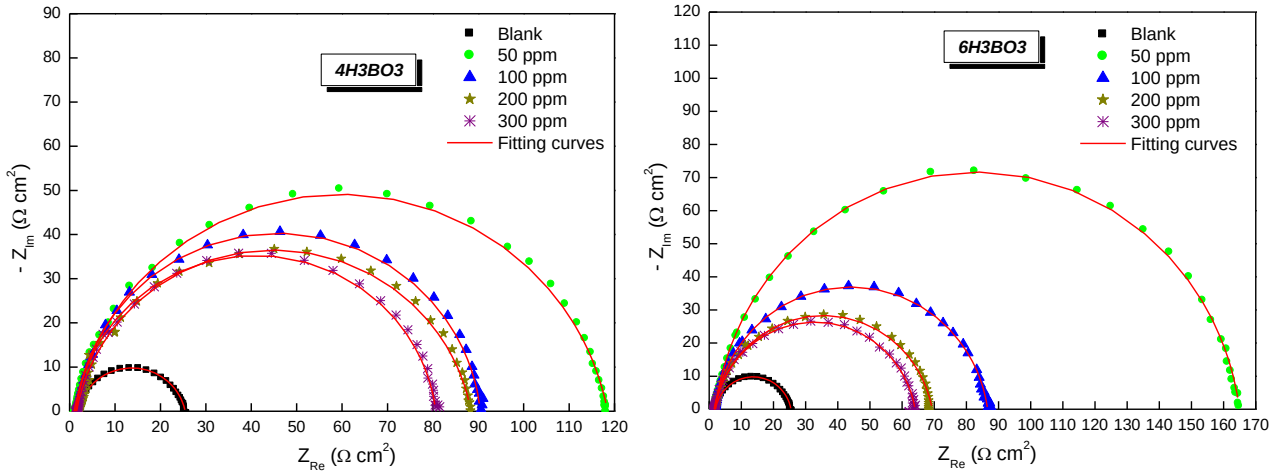

Fig. 2. Nyquist plots for steel/HCl electrochemical systems without and after adding different concentrations of $4H_3BO_3$ (a) and $6H_3BO_3$(b).

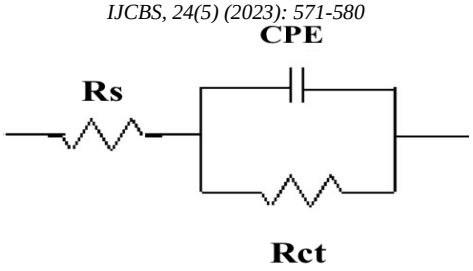

Fig. 3. Equivalent electrical circuitry utilized to model experimental (EIS) data

Fig. 4. Bode plots of mild steel/HCl electrochemical system at different concentrations of $4H_3BO_3$ (a) and $6H_3BO_3$(b)

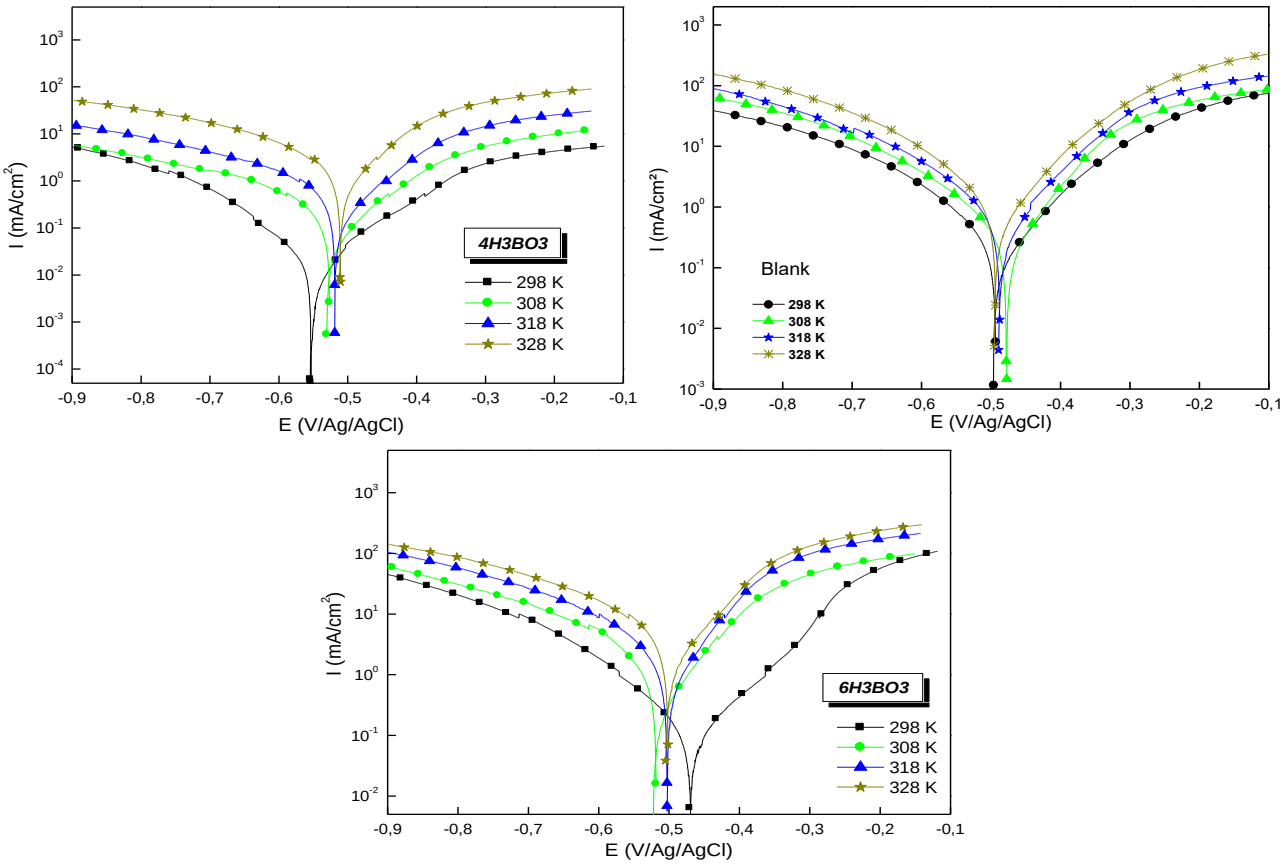

Fig. 5. Polarization curves of mild steel in 1 M HCl in the absence and presence of 50 ppm of $4H_3BO_3$ and $6H_3BO_3$ at different temperatures

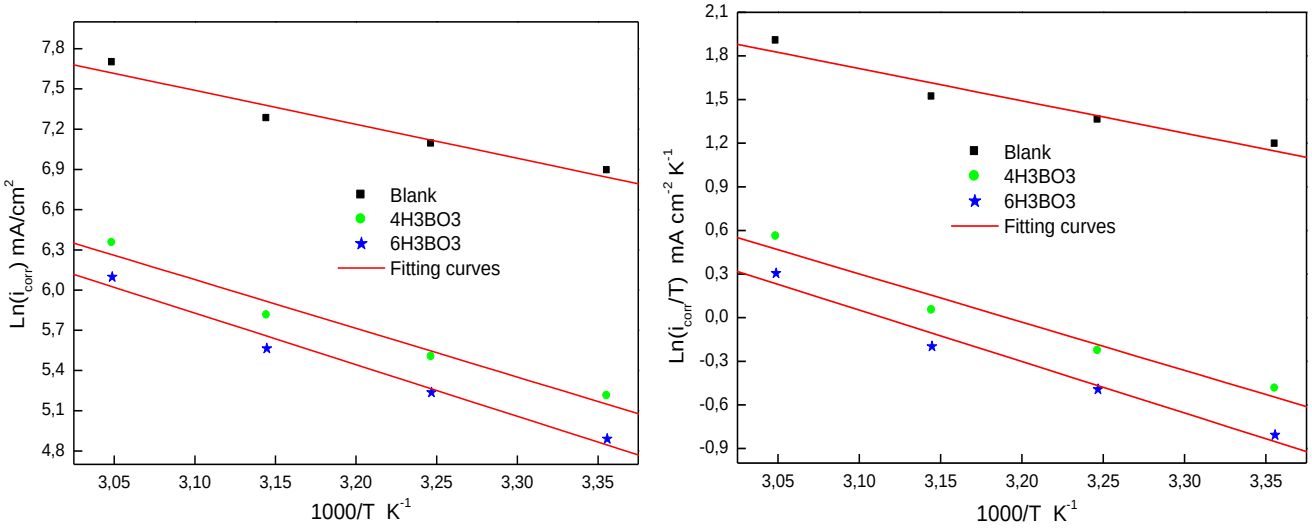

Fig. 6. Arrhenius diagrams for mild steel in HCl 1,0 M in the absence and the presence of 50 ppm of both glassy compounds/(a) of ln (i_{corr}) *vs.* 1000/T and (b) ln(i_{corr}/T) *vs.* 1000/T

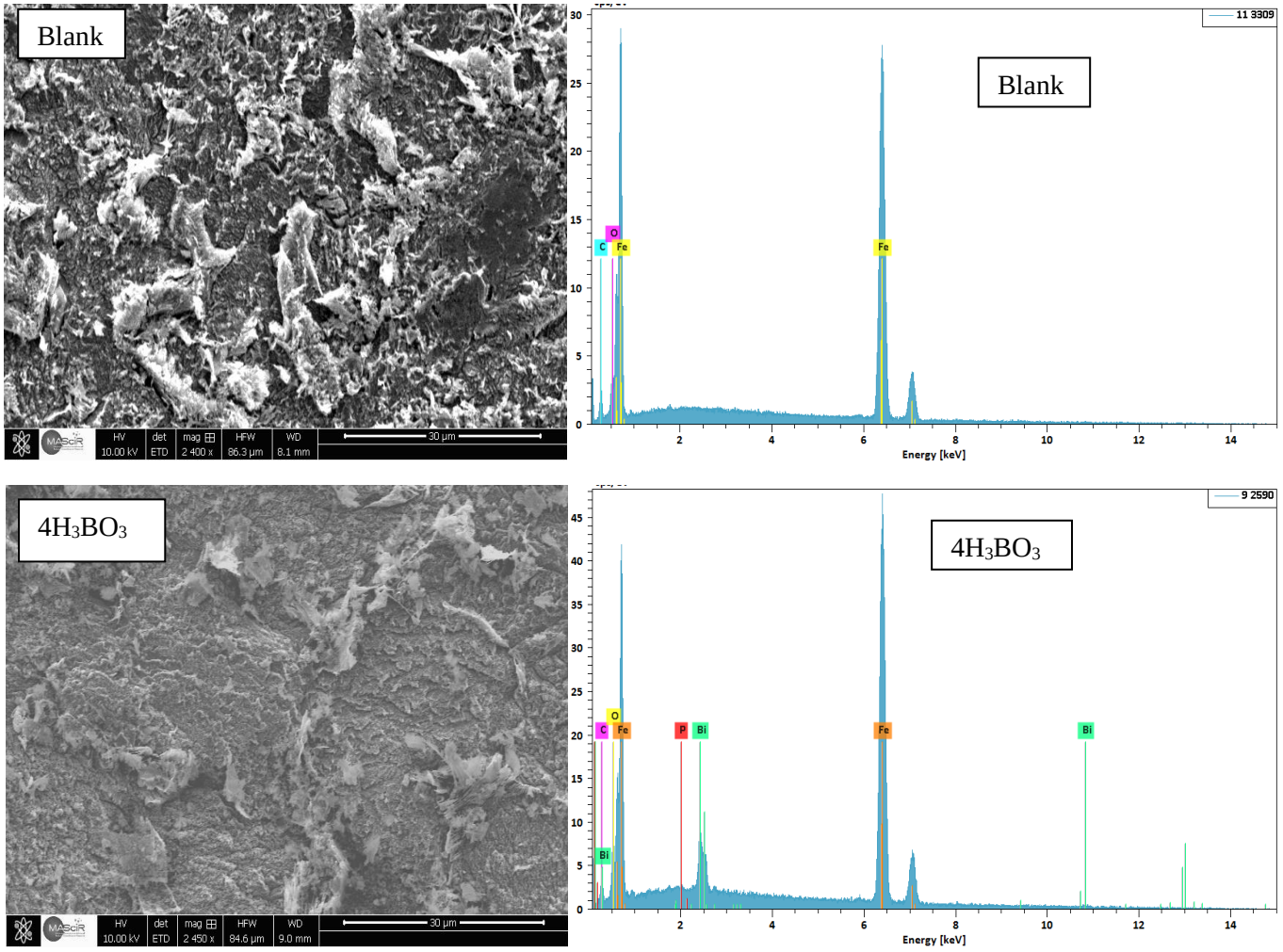

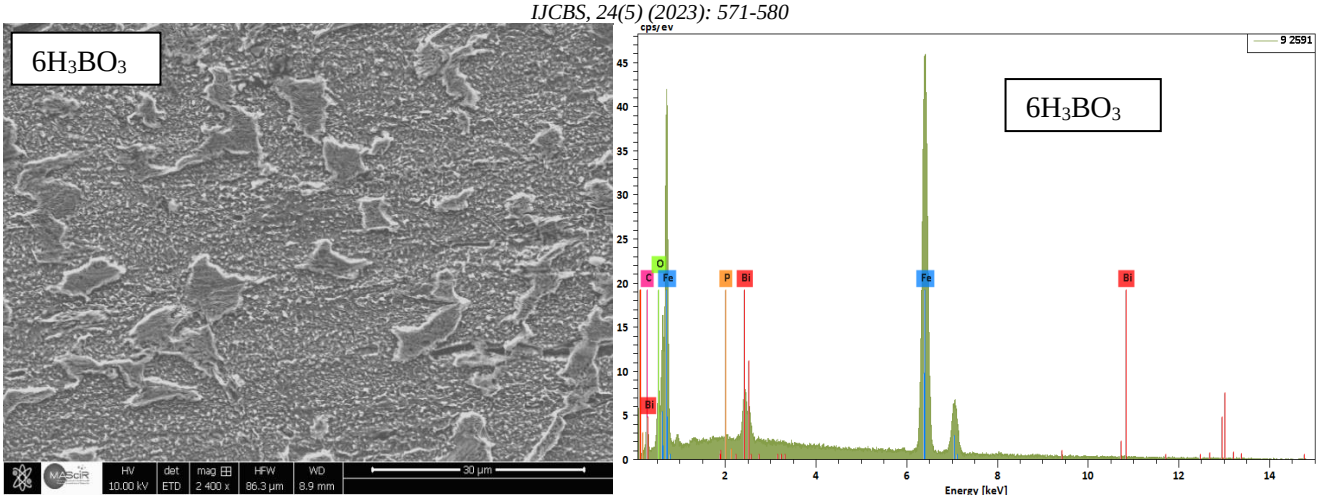

Fig. 7. SEM micrographs of both uninhibited (Blank) and inhibited MS (after the addition of 50 ppm of $4H_3BO_3$ and $6H_3BO_3$) at 298 K

The impedance function of CPE can be described by the expression [37]:

$$Z_{CPE} = \frac{1}{Q(i\omega)^n}$$

where Q is the magnitude of the CPE, j is the imaginary number, ω is the angular frequency, and n can be used as an index of the surface homogeneity ($-1 < n < +1$), When n = 0, − 1, and 1, CPE represent resistor, inductor, and pure capacitor, respectively. The double-layer capacitance (Cdl) is obtained by the following formula [38]:

$$C_{dl} = \frac{\varepsilon \varepsilon_0 s}{e}$$

Where Ɛ and $Ɛ_o$ represent the dielectric constants of the medium and permittivity under vacuum, e represents the thickness of the protective layer and S correspond to the electrode surface. From Table 3, the values of Rt become more extensive with the decrease of the concentration of both inhibitors and which holds a higher value at 50 ppm, which means a reduction in the rate of corrosion. The inhibitory efficacy E (%), of these inhibitors, evolves in the same way as Rt and achieves a better inhibitory efficiency is equal to 80,0% and 86,5% to 50 ppm for both $4H_3BO_3$ and $6H_3BO_3$ compounds respectively. Moreover, the value of the proportional factor Q of CPE varies in the usual way with the concentration of $4H_3BO_3$ and $6H_3BO_3$. This is attributed to the increase in surface coverage of mild steel by the inhibitory molecules leading to increased inhibition efficiency [39]. The increase in Rct value is attributed to the formation of a protective layer in the metal/solution interface.

According to the Bode diagrams (Fig. 4), there is only one maximum. The height of this peak decreases with the concentration of $4H_3BO_3$ and $6H_3BO_3$ revealing the strong adsorption of $4H_3BO_3$ and $6H_3BO_3$ on the steel surface [40]. Also, the log|Z| values were significantly enhanced at low frequency with decreasing inhibitor concentration and the shape of the plots remained unchanged in the presence of $4H_3BO_3$ and $6H_3BO_3$.

3.3. Effect of temperature and thermodynamic parameters

Generally, temperature is one of the factors that can influence the electrochemical behavior of metals in a corrosive environment [41]. Therefore, it becomes necessary to ensure the inhibition ability of both studied molecules at higher temperatures. In order to determine the effect of this variable on the inhibitory power of both glassy compounds ($4H_3BO_3$ and $6H_3BO_3$) on mild steel, we performed stationary electrochemical characterization in potentiostatic mode at different temperatures (298 K to 328 K). The polarization plots obtained in HCl 1.0 M without and with the addition of 50 ppm of the tested compounds in the temperature range (298-328 K) are presented in Figure 5. The choice of concentration 50 ppm is justified by the fact that at this concentration, the value of the efficiency is maximum. The values of the corrosion current densities (I_{corr}), corrosion potentials of the steel (E_{corr}) and the inhibition efficiencies as a function of temperature are given in Table 4.

It is remarked that these curves exhibited the Tafel regions. It is noted also that the anodic and cathodic branches increased with increasing of temperature. The curves in the cathodic part are parallel, indicating that the reduction of H+ ions on the steel surface is done according to the same pure activation mechanism in all temperature range. The corrosion potential E_{corr} for the different temperatures shifts slightly towards the cathodic values in the presence of $6H_3BO_3$ but in the presence of $4H_3BO_3$ the corrosion potential E_{corr} shifts slightly toward the anodic values. The Inhibition efficiency ηPP (%) of the tested compounds decreases with the temperature increase. This can be explained by the positive contribution to the corrosion phenomenon. This can be also explained by a slight change of equilibrium adsorption-desorption in favor of the desorption process thus decreasing the inhibitory power of the molecule [42,43].

To further understand the type of inhibitor adsorption, the variations of the logarithm of the corrosion current density as a function of the inverse of temperature (1000/T) were plotted and displayed in Fig.6. The variation of ln (i_{corr}) = f (1000/T) is linear. The slope of the obtained lines is used to determine the activation energy (Ea) values which was calculated according to the Arrhenius expression [44].

$$i_{corr} = Aexp(\frac{-E_a}{RT})$$

where i_{corr} denotes the corrosion current density, A is a pre-exponential factor, R is the ideal gas constant and T represents the absolute temperature (K). The values of enthalpy of activation (ΔHa) and entropy of activation (ΔSa)

can be calculated from the alternative form of Arrhenius equation as follows [45]:

$$i_{corr} = \frac{RT}{Nh} exp(\frac{\Delta S_a}{R}) xp(-\frac{\Delta H_a}{RT})$$

where h represents the Planck Constant, N is the Avogadro number. Fig. 6 shows the evolution of ln(icorr/T) as a function of the inverse of the temperature in the form of a straight line with a slope of (− ΔHa/R). The extrapolation of these lines gives the values of (Ln (R/Nh) + ΔSa/R), thus those of ΔHa and ΔSa. The obtained results are listed in Table 6. Table 5 shows an increase in the activation energy (Ea) values before (Blank) and after the addition of both glassy compounds. This increase suggests that these inhibitors are physically adsorbed on the metal surface [46]. Indeed, a higher energy barrier to the corrosion process in the inhibited solution is associated with the formation of a weak chemical bond between the inhibitory molecules and the mild steel surface [47]. ΔSa in the presence of 50 pmm of these inhibitors in solution compared to the case of the blank acid solution might be due to the enhanced randomness of the molecules [48,49].

3.4. Scanning electron Microscopy (SEM)

SEM analysis was employed to explore the surface morphology of MS samples immersed for 6 h in 1.0 M HCl alone as well as in the presence of the studied products. Fig. 7 shows SEM images of MS plates after immersion in the corrosive medium alone and in the corrosive solution containing $4H_3BO_3$ and $6H_3BO_3$. The morphology of the examined metal after immersion in the corrosive solution alone (Blank), the steel surface is highly corroded due to the dissolution of the metal [50]. Whereas the surface becomes smoother after the addition of 50 ppm of both glassy compounds $4H_3BO_3$ and $6H_3BO_3$ as illustrated in Fig.7 This observation shows that the inhibition is due to the formation of a stable and insoluble adhesive deposit that restricts electrolyte access to the surface of the steel. We realized EDX analyses in order to identify the different elements present on the mild steel surface (Table 6). Figure 7 presents EDX spectrums. In the case of the blank, we note the formation of iron oxide and the apparition of an oxygen peak, emerging from the steel attack in HCl 1.0 M.

We note also, in the presence of $4H_3BO_3$ and $6H_3BO_3$, a decrease in the carbon and oxygen peak and the presence of Bismuth and fluorine. These observations confirm that the glassy compounds decrease the steel corrosion by forming a layer, which restricts electrolyte access to the surface of the steel.

4. Conclusions

In the experimental part, it has been clearly demonstrated that all the techniques used, are capable to characterize and to follow the corrosion inhibition process promoted by two glassy compounds: $4H_3BO_3$ and $6H_3BO_3$ was investigated. The corrosion inhibition of mild steel in 1.0 M HCl by these glassy compounds was studied using electrochemical measurements. The effect of the inhibitor concentration and the aggressive solution temperature on corrosion behavior was investigated. Hence, the following conclusions are drawn:

- The overall results indicate that these compounds act as effective corrosion inhibitors for mild steel in 1.0 M HCl solution, with an efficiency that depends on the inhibitor concentration and temperature of the medium. The performance decreases with concentration to reach a maximum inhibition efficiency (over 86%) at 50 ppm at 298 K.
- It is also observed that the mechanism of hydrogen reduction and iron dissolution is modified by the addition of the studied inhibitors. The adsorption mechanism on the surface of the metal and its inhibition can depend on the nature of the crystal structure and the phases present in these inhibitors.
- The inhibition efficiency was found in the order: $6H_3BO_3$ > $4H_3BO_3$ and the inhibition efficiencies determined by potentiodynamic polarization and EIS methods are in good agreement with each other.
- The study of temperature effect on the inhibition efficiency shows that this one decreases with the temperature increase.
- Surface morphology studies confirmed the mitigation of mild steel corrosion by the formation of a protective film on the surface of the steel.

References

[1] C. Verma, M.A. Quraish. (2021). Recent progresses in Schiff bases as aqueous phase corrosion inhibitors: Design and applications. Coordination Chemistry Reviews. 446: 214105

[2] E. Berdimurodov, I. Eliboyev, K. Berdimuradov, A. Kholikov, K. Akbarov, O. Dagdag, N. Arrousse. (2022). Green β-cyclodextrin-based corrosion inhibitors: Recent developments, innovations, and future opportunities. Carbohydrate Polymers. 292: 119719.

[3] M.A. Quraishi, D.S. Chauhan, V.S. Saji. (2021). Heterocyclic biomolecules as green corrosion inhibitors, Journal of Molecular Liquids. 341: 117265.

[4] M. Ouakki, M. Galai, M. Cherkaoui. (2022). Imidazole derivatives as efficient and potential class of corrosion inhibitors for metals and alloys in aqueous electrolytes: A review. Journal of Molecular Liquids. 345: 117815.

[5] A. Elbadaoui, M. Galai, S. Ferraa, H. Barebita, M. Cherkaoui, T. Guedira. (2019). A new family of borated glasses as a corrosion inhibitor for carbon steel in acidic medium (1.0 M HCl). Analytical and Bioanalytical Electrochemistry. 11 (1): 19–37.

[6] A.A. Aghzzaf, B. Rhouta, E. Rocca, A. Khalil, J. Steinmetz. (2014). Corrosion inhibition of zinc by calcium exchanged beidellite clay mineral: a new smart corrosion inhibitor. Corrosion Science. 80: 46–52.

[7] F. Atmani, D. Lahem, M. Poelman, C. Buess-Herman, M.G. Olivier. (2013). Mild steel corrosion in chloride environment: effect of surface preparation andinfluence of inorganic inhibitors. Corrosion Engineering Science and Technology. 48: 9–18.

[8] M. Boudalia, A. Guenbour, A. Bellaouchou, A. Zarrouk. (2015). New eco-friendly corrosion inhibitor: inhibitive and adsorption action of clay for the corrosion of stainless steel in H_3PO_4 solutions. Der Pharma Chemica. 7: 301–306.

[9] D. Nan, S. Wang, Z. Qing, Z. Shao. (2012). Effects of boric acid on microstructure andcorrosion

resistance of boric/sulfuric acid anodic film on 7050 aluminum alloy. Transactions of Nonferrous Metals Society of China. 22: 1655–1660.

[10] V. Moutarlier, M.P. Gigandet, J. Pagetti, S. Linget. (2005). Influence of molybdatespecies added to sulphuric acid on composition and morphology of the anodiclayers formed on 2024 aluminium alloy. Thin Solid Films. 483 (1-2): 197–204.

[11] M. Mohammadi, A.Yazdani, M. E. Bahrololoom, A. fantazi. (2013). Corrosion behavior of 2024 aluminum alloy anodized in presence of permanganate and phosphate ions. Journal of Coating Technology and Research. 10: 219–229.

[12] H. El Boulifi, M. Ouakki, H. Barebita, T. Guedira, and M. Cherkaoui. (2021). Assessing the corrosion inhibition performance of two borate-based glasses for mild steel in hydrochloric acid. Materials Today: Proceedings. 37: 3967–3972.

[13] M. Laourayed, M. El Moudane, M. Khachani, M. Boudalia, A. Guenbour, A. Bellaouchou, A. Zarrouk. (2019). Thermal, structural and corrosion inhibition performances of a new phosphate glasses on mild steel in HCl medium. Chemical Data Collections. 24: 100305.

[14] A. Elbadaoui, M. Galai, S. Ferraa, H. Barebita, M. Cherkaoui, T. Guedira. (2019). Effect of bismuth and bore content in glass system inhibitor on the corrosion behavior of mild steel in 1M hydrochloric acid solution. Mediterranean Journal of Chemistry. 8 (4): 328–337.

[15] A. Shaim, M. Galai, E. Amaterz, A. Benlhachemi, M.E. Touhami, A. Chahine. (2019). Titan content in glass system inhibitor effect on the corrosion behavior of mild steel in 3% NaCl medium. Analytical, Bioanalytical, and Electrochemistry. 11: 522–534.

[16] L. Feng, H. Yang, F. Wang. (2011). Experimental and theoretical studies for corrosion inhibition of carbon steel by imidazoline derivative in 5% NaCl saturated $Ca(OH)_2$ solution. Electrochimica Acta. 58: 427–436.

[17] M.M. Mennucci, E.P. Banczek, P.R.P. Rodrigues, I. Costa. (2009). Evaluation of benzotriazole as corrosion inhibitor for carbon steel in simulated pore solution. Cement and Concrete Composites. 31: 418–424.

[18] K. Haruna, L.M. Alhems, T.A. Saleh. (2021). Graphene oxide grafted with dopamine as an efficient corrosion inhibitor for oil well acidizing environments. Surfaces and Interfaces. 24: 2468–10230.

[19] A. Saleh. Tawfik, K. Haruna, A. Rashid, I. Mohammed. (2021). Octanoate grafted graphene oxide as an effective inhibitor against oil well acidizing corrosion, Journal of Molecular Liquids. 325: 115060.

[20] K. Haruna, T.A. Saleh. (2021). N,N′-Bis-(2-aminoethyl)piperazine functionalized graphene oxide (NAEP-GO) as an effective green corrosion inhibitor for simulated acidizing environment. Journal of Environmental Chemical Engineering. 9: 104967.

[21] K. Haruna, T.A. Saleh, M.A. Quraishi. (2020). Expired metformin drug as green corrosion inhibitor for simulated oil/gas well acidizing environment. Journal of Molecular Liquids. 315: 113716.

[22] G. Ghenimi, M. Ouakki, H. Barebita, A. El Fazazi, T. Guedira, M. Cherkaoui. (2020). New Vitreous Phase as Mild Steel Inhibitors in Hydrochloric Acid. Analytical, Bioanalytical, and Electrochemistry. 12(1): 1-20.

[23] B. Baach, M. Ouakki, S. Ferraa, H. Barebita, M. Cherkaoui, A. Nimour, T. Guedira. (2022). Experimental evaluation of new inorganic compounds based on bismuth oxide Bi_2O_3 as corrosion inhibition for mild steel in acidic medium. Inorganic Chemistry Communications. 137: 109233.

[24] El. Azeddine, M. Galai, S. Ferraa, H. Barebita, M. Cherkaoui, T. Guedira. (2019). Effect of bismuth and bore content in glass system inhibitor on the corrosion behavior of mild steel in 1M hydrochloric acid solution. Mediterranean Journal of Chemistry. 8 (4): 328-337.

[25] M. Belfaquir, T. Guedira, S.M.D. Elyoubi, and J.L. Rehspringer. (2013). Science Lib Editions Mersenn. 5: 130303.

[26] A. Elbadaoui, M. Galai, M. Cherkaoui, and T. Guedira. (2016). Der Pharma Chem. 8: 214.

[27] C. Verma, L.O. Olasunkanmi, E.D. Akpan, M.A. Quraishi, O. Dagdag, M. El Gouri, El-Sayed M. Sherif, E.E. Ebenso. (2020). Epoxy resins as anticorrosive polymeric materials: a review. Reactive and Functional Polymers. 104741.

[28] I.B. Obot, N.O. Obi-Egbedi, and N.W. Odozi, (2010). Acenaphtho [1, 2-b] quinoxaline as a novel corrosion inhibitor for mild steel in 0.5 M H2SO4. Corrosion Science. 52: 923.

[29] M. Ouakki, M. Rbaa, M. Galai, B. Lakhrissi, E. H. Rifi, and M. Cherkaoui. (2018). Experimental and quantum chemical investigation of imidazole derivatives as corrosion inhibitors on mild steel in 1.0 M hydrochloric acid. Journal of Bio- and Tribo-Corrosion. 4: 35.

[30] E. Ech-chihbi, M. E. Belghiti, R. Salim, H. Oudda, M. Taleb, N. Benchat, B. Hammouti, and F. El-Hajjaji. (2017). Journal of Surfaces and Interfaces. 9: 206.

[31] R.A. Prabhu, T.V. Venkatesha, B.M. Praveen, K.G. Chandrappa, and S.B. Abd Hamid. (2012). Transactions of Indian Institute of Metals. 67: 675

[32] D. Frenkel, and B. Smit. (2002). Understanding Molecular Simulation: From Algorithms to Applications, 2nd Ed, Academic Press, San Diego.

[33] M. Galai, M. Rbaa, Y. El Kacimi, M. Ouakki, N. Dkhirech, R. Touir, B. Lakhrissi, and M. Ebn Touhami. (2017). Anti-corrosion Properties of some Triphenylimidazole Substituted Compounds in Corrosion Inhibition of Carbon Steel in 1.0 M Hydrochloric Acid Solution. Analytical, Bioanalytical, and Electrochemistry. 9: 80.

[34] M. Ouakki, M. Galai, Z. Benzekri, Z. Aribou, E. Ech-chihbi, L. Guo, K. Dahmani, K. Nouneh, S. Briche, S. Boukhris, M. Cherkaoui. (2021). A detailed investigation on the corrosion inhibition effect of by newly synthe- sized Pyran derivative on mild steel in 1.0 M HCl: Experimental, surface mor-phological (SEM-EDS, DRX& AFM) and

computational analysis (DFT & MD simulation), Journal of Molecular Liquids. 344: 117777

[35] G. Sıgˇırcık, D. Yildirim, T. Tüken. (2017). Synthesis and inhibitory effect of N, N'-bis (1-phenylethanol) ethylenediamine against steel corrosion in HCl Media. Corrosion Science. 120: 184–193.

[36] F. El kalai, T. Chelfi, N. Benchat, M. Bouklah, S. Daoui, K. Karrouchi, M. Allali, M. Taleb, E. Ech–chihbi, F.A. Almalki, T.B. Hadda, (2020). New Heterocyclic Compounds Based on Pyridazinones Scaffold as Efficient Inhibitor of Corrosion of Mild Steel in Acidic Solution 1 M HCl, Journal of Bio- and Tribo-Corrosion. 6: 89.

[37] S. Ferraa, M. Ouakki, H. Barebita, A. Nimour, M. Cherkaoui, T. Guedira. (2021). Corrosion inhibition potentials of some phosphovanadate-based glasses on mild steel in 1 M HCl. Inorganic Chemistry Communications. 132: 108806.

[38] Y. El Kacimi, R. Touir, K. Alaoui, S. Kaya, A. Salem Abousalem, M. Ouakki, M. Ebn Touhami. (2020). Anti-corrosion properties of 2-phenyl-4(3H)-quinazolinone-substituted compounds: electrochemical, quantum chemical, monte carlo, and molecular dynamic simulation investigation, Journal of Bio- and Tribo-Corrosion. 6: 47.

[39] X. Zheng, S. Zhang, W. Li, L. Yin, J. He, and J. Wua. (2014). Investigation of 1-butyl-3-methyl-1H-benzimidazolium iodide as inhibitor for mild steel in sulfuric acid solution. Corros. Sci. 80: 383.

[40] R. Yıldız, A. Döner, T. Dogˇan, I. Dehri. (2014). Experimental studies of 2- pyridinecarbonitrile as corrosion inhibitor for mild steel in hydrochloric acid solution. Corrosion Science. 82: 125–132.

[41] P. Singh, D.S. Chauhan, S.S. Chauhan, G. Singh, M.A. Quraishi. (2020). Bioinspired synergistic formulation from dihydropyrimdinones and iodide ions for corrosion inhibition of carbon steel in sulphuric acid. Journal of Molecular Liquids. 298: 112051. https://doi.org/10.1016/j.molliq.2019.112051

[42] I. B. Obot, and N. O. Obi-Egbedi. (2010). Theoretical study of benzimidazole and its derivatives and their potential activity as corrosion inhibitors. Corros. Sci. 52: 657.

[43] G. N. Mu, X. Li, and F. Li. (2004). Synergistic inhibition between o-phenanthroline and chloride ion on cold rolled steel corrosion in phosphoric acid. Mater. Chem. Phys. 86: 59

[44] K. Dahmani, M. Galai, M. Cherkaoui, A. Elhasnaoui, A. El Hessni. (2017). Journal of Material and Environmental Science. 8: 1676–1689.

[45] L. Afia, R. Salghi, A. Zarrouk, H. Zarrok, O. Benali, B. Hammouti, L. Bazzi. (2015). Inhibitive action of argan press cake extract on the corrosion of steel in acidic media, Portugaliae. Electrochimica Acta. 30 (4): 267–279.

[46] C. Verma, M.A. Quraishi, A. Singh. (2015). 2-Amino-5-nitro-4, 6-diarylcyclohex-1-ene-1, 3, 3-tricarbonitriles as new and effective corrosion inhibitors for mild steel in 1 M HCl: Experimental and theoretical studies. Journal of Molecular Liquids. 212: 804

[47] A. Popova, E. Sokolova, S. Raicheva, M. Christov. (2003). AC and DC study of the temperature effect on mild steel corrosion in acid media in the presence of benzimidazole derivatives. Corrosion Science. 45: 33–58.

[48] A. Salhi, S. Tighadouini, M. El-Massaoudi, M. Elbelghiti, A. Bouyanzer, S. Radi, S. El Barkany, F. Bentiss, A. Zarrouk. (2017). Keto-enol heterocycles as new compounds of corrosion inhibitors for carbon steel in 1 M HCl: Weight loss, electrochemical and quantum chemical investigation. Journal of Molecular Liquids. 248: 340–349.

[49] M. Galai, M. Rbaa, Y. El Kacimi, M. Ouakki, N. Dkhirech, R. Touir, B. Lakhrissi, M. Ebn Touhami. (2017). Anti-corrosion Properties of some Triphenylimidazole Substituted Compounds in Corrosion Inhibition of Carbon Steel in 1.0 M Hydrochloric Acid Solution. Analytical, Bioanalytical, and Electrochemistry. 9: 80–101.

[50] N. El Hamdani, R. Fdil, M. Tourabi, C. Jama, F. Bentiss. (2015). Alkaloids extract of Retamamonosperma (L.) Boiss. seeds used as novel eco-friendly inhibitor for carbon steel corrosion in 1 M HCl solution: Electrochemical and surface studies. Applications of Surface Science. 357: 1294–1305.